I.A.U
Karaj branch

Journal of
A p p l ied
C hemical
R esearch
jacr.kiau.ac.ir

*Journal of Applied Chemical Research, 17, 3, 52-68 (2023)*

# A Facile Strategy for Synthesis of Well-defined Polypropylene-grafted-polystyrene /MMT Nanocomposite Using Reversible Addition: Fragmentation Chain Transfer Polymerization and Solution Intercalated Method

**Saber Ghasemi Karaj-Abad[1], Parisa Shamsno[1], Mojtaba Abbasian[2], Mehdi Hosseinzadeh[3*] Solmaz Esmaeily Shoja[4]**

*[1]Department of Chemistry, Payame Noor University, Tehran, Iran*

*[2]Department of Chemical Engineering, University of Bonab, Bonab, Iran*

*[3]Marand Faculty of Technical and Engineering, University of Tabriz, Tabriz, Iran*

*[4]Faculty of Engineering, Islamic Azad University, Bonab Branch, Bonab, Iran*

*(Received 15 Nov. 2022; Final revision received 15 Feb. 2023)*

**Abstract**

A simple and easy synthetic route for preparing PP-*g*-PSt/O-MMt nanocomposite was synthesized using a combination of ring-opening polymerization and reversible addition–fragmentation chain transfer polymerization techniques. Firstly, MAH (maleic anhydride) was reacted with PP (polypropylene) followed by the opening of an anhydride ring with ethanolamine to obtain a hydroxyl group including polypropylene (iPP-OH). Secondly, the produced PP-OH was treated with 4-cyano-4-[(phenylcarbothioyl) sulfanyl] pentanoic acid– to synthesize of PP-RAFT macroinitiator. Then, the styrene monomer was grafted onto PP using RAFT approach to produce a well-defined (PP-*g*-PSt) copolymer. Finally, Polymer/clay nanocomposite was synthesized through a solution intercalation method. The successful synthesis of all materials was proved using FT-IR and $^{1}$H NMR spectroscopy. The structural morphology and thermal properties of the grafted copolymer /O-MMT nanocomposite were examined using SEM, TGA, and DSC. This approach employed via the RAFT method is an easy and alternative strategy for synthesizing new materials.

**Keywords**: Graft copolymer, Polystyrene, Polypropylene, RAFT polymerization, Nanocomposite.

***Corresponding author**: Mehdi Hosseinzadeh, Marand Faculty of Technical and Engineering, University of Tabriz, Tabriz, Iran. E-mail addresses: mh_1268@yahoo.com.*

## Introduction

Polypropylene is the second widely used thermoplastic in the group of polyolefins. Polypropylene was firstly introduced by Giulio Natta in 1945 and now approximately 21% of the global consumption of basic polymers is attributed to Polypropylene. PP (polypropylene) is a wide spreading utilized thermoplastic polymer that employs in packing [1], manufacturing [2], and the automotive construction industry [3], among others. Nevertheless, its unique features necessitate its alteration to achieve the favorable features.

Generally, PP is modified by blending or grafting with another polymer. Grafting or blending techniques are effective, facile and economical techniques for providing materials with excellent features. A blend or graft of PP with PSt (Polystyrene) is more attractive, because PSt is preferable toward pure PP during its HDT (heat deflection temperature) and hardness. As a result, blending or grafting these two polymers has the potential to achieve a material with a high HDT and hardness than pure PP. On the other hand, Polyolefin/Polystyrene (PSt) blends in a comparison to other immiscible polymer blends, suffer from low interfacial interaction, which leads to undesirable mechanical and thermal properties [4-6].

Typically, Graft copolymers have been prepared by macro-monomer approaches [7-10]. The attachment of two different polymers using a reaction of coupling [11], or through the polymerization of a monomer from activity portions on a polymer chain [12,13] further research has focused on end-functional polymers to preparing graft and block copolymers, polymer networks and star polymers. Star and graft methods that have correctly controlled macromolecular architecture are demonstrated to be beneficial to control rheology factors, compatible with emulsifiers and polymer blends [14].

Nowadays, among nanocomposites, more attention has been paid to polymer based-on nanocomposites. Polymer nanocomposite developed with well-dispersed layered silicate, commonly montmorillonite has received much consideration in both industrial and scientific research because of its small size and extraordinary properties in comparison to traditional filler composite materials. One of the reasons for developing polymer based on nanocomposites is their excellent chemical, physical and mechanical features. In general, the polymers based-on nanocomposites have low gravity, great rigidity, high thermal stability, good electrical conductivity, unique chemical resistance and fire retardancy, magnetic and electric properties in comparison with the bulk polymers [15-17].

The growth of controlled/living polymerizations has allowed synthetic polymer chemists to propose complex polymeric buildings with high accuracy [18]. On the other hand, living radical polymerization demonstrates a significant role in the preparation of various polymeric

materials. This method is executable in various monomers, also its mechanism is relatively facile and free radical polymerization methods are accurately known. Thus, the synthesis of various copolymers has received more and more attention owning to their capability to prepare polymeric materials based-on well-controlled molecular weights, well-defined structure, macromolecular architectures and also low dispersion under relatively easy and feasible experimental conditions [19, 20].

Different methods for CRP have been offered. However, in the few last decades, a great advancement of methods has been created in living/controlled radical polymerizations, including atom transfer radical polymerization (ATRP) [21-23], reversible addition fragmentation transfer polymerization (RAFT) process [24,25], and nitroxide-mediated polymerization (NMP) [26,27]. Among these basic techniques, RAFT demonstrates the most useful and facile method, since it uses a diversity of chain transfer agents [28] allowing a broad range of monomers to be polymerized without using transition metal catalysts. RAFT polymerization is a more facile and strong method for the synthesis of various types of macromolecules and water-soluble polymers with favorite molecular design and functionality, as it can be applied to almost any type of monomer without the necessity of employing protecting functional groups. As a result, it is possible to control low polydispersity and high molecular weight during the reaction and a chain polymerization by RAFT agent or CTA (reversible = deactivation chain transfer agent) [29].

RAFT approach is popular for production of novel materials with different features. The main reason for high performance of RAFT polymerization is its independence on metal catalysts that enables it to be done in various ranges of reaction conditions like temperature and solvents. Also, a wide range of monomers with and without functional groups (OH, $NR_2$, COOH, and $CONR_2$) have been polymerized via this polymerization method [12]. Dithiocarbonyl compounds are a kind of RAFT polymerization agent. By choosing a suitable R and Z groups, RAFT agent [ZC5S (SR)] can be used successfully for the synthesis of polymers with narrow polydispersity index and predetermined MW [14].

In this present research work, a typical method for synthesizing a PP-*g*-PSt/O-MMt nanocomposite *via* a combination of RAFT polymerization and solution methods was examined. In this method, maleic anhydride was reacted with polypropylene (PP) followed by opening of anhydride ring with ethanolamine to obtain a hydroxyl group containing polypropylene (PP-OH). After that, the produced PP-OH was modified with RAFT agent to synthesize an initiator that can polymerize styrene by RAFT technique. Finally, (PP-*g*-PSt)/O-MMt nanocomposite is synthesized by solution intercalation method. The properties of

polymer/clay nanocomposite (morphology and thermal behavior) relations were demonstrated by Fourier transform infrared (FT-IR) spectroscopy, SEM and DSC/TGA. Many advantages of PP-g-PSt/clay nanocomposite have been reported including their mechanical properties, thermal properties, permeability, uniform dispersion of inorganic nanoparticles into the matrix, and synthesis of nanocomposite with well-defined structure and biomedical applications [30]. Consequently, PP-g-PSt/clay nanocomposite has enormous potential for application in the automobile, airplane, satellite, biomedical, and other polymer industries where the enhancement of the mechanical, permeability, or thermal properties of polymers is important.

## Experimental

*Materials*

The RAFT chain transfer agent (CTA) 4-cyano-4- [(phenylcarbothioyl) sulfonic] pentatonic acid was synthesized [31]. Bis(thiobenzoyl) disulfide was prepared according to the reported method by Le et al. [32]. Carbon disulfide was dried with calcium chloride, and then distilled. Bromobenzene was dried with calcium chloride and distilled before use. THF (tetrahydrofuran) and Toluene (Merck, Darmstadt, Germany) was dried by refluxing over sodium wire, then distilled under argon flowing before use. The 2,2ˈ-azobis (2-methylpropionitrile) initiator (AIBN; Switzerland, Fluka) were acquired from Sigma-Aldrich (Louis. St, USA, MO) and recrystallized from ethanol at 50 °C prior to use.

4-dimethyleaminopyridine (DMAP) and 1, 3-dicyclohexylcarbodiimide (DCC), with purity of %99 was acquired from Merck and were used as received. Hexadecyl trimethyl ammonium chloride salt was provided from Merck. $Na^+$-MMT (Sodium montmorillonite) was prepared from Southern Clay Products (USA, TX, Gonzales), under the brand of Cloisite NaC, with a cation exchange capacity of 95 meq/100 g and an idealized chemical formula of $Na_{0.33}[Mg_{0.33}Al_{11.67}Si_4O_{10}](OH)_2$. Styrene monomer was provided from Tabriz Petrochemical Company (T.P.C) (Tabriz, Iran). It was dried over calcium hydride ($CaH_2$), distilled under reduced pressure from $CaH_2$ and then kept at −20 °C before use. Isotactic polypropylene (iPP) was provided by Tabriz Polynar Co. (Tabriz, Iran) and used without purification. MA (Maleic anhydride), Ethanolamine, *O*-Xylene (Merck), triethylamine and BPy (2, 2′-bipyridine) were acquired (Aldrich-Sigma Co.) and utilized as received. All other solvents and chemical materials were acquired from Merck or sigma-Aldrich and refined according to the literature.

*Characterization and analyses*

The specimens of FTIR spectrum were obtained on a Bruker IFS 55 FTIR apparatus within the range of 400–to-4000 $cm^{-1}$ with 128 scans and a spectral resolution of 4 $cm^{-1}$. Each specimen was recorded by means of dry powders with KBr pellets and the mixture was compressed into pellets. To remove humidity absorption, pellets were kept in a desiccator. $^1H$ NMR spectrum were provided at 25 $^oC$ employing a Fourier transform NMR (F: 300 MHz) Brucker apparatus (Germany, Ettlingen, Brucker). The specimen for $^1H$ NMR spectroscopy was obtained by dissolving about 15 mg of findings in 10 ml of deuterated dimethyl sulfoxide or $CDCl_3$. SEM (scanning electron microscopy) was carried out by means of CAM SCAN MV 2300 - Hitachi apparatus without gold coverage at 10KV. The thermal behaviors of the resultant nanocomposites were performed with a TGA-SDTA $851^0$ (Shropshire, UK, Polymer Laboratories). Almost 15 mg of the material was heated at 30 to 700 $^oC$ under nitrogen flow rate of 10 $^oC$/min. DSC analysis was employed with a Mettler/Toledo (Germany, Selb)-DSC 822 e. First, the specimen was heated under a flowing $N_2$ to 250 $^oC$ and in order to remove the thermal history, allowed to cool for about 5 minutes. Afterward, the material was recovered after the heating rate of 10 $^oC$/min. The overall investigation was carried out under $N_2$ pouring at a flow rate of 50 ml min.

*Synthesis of iPP-g- MAH*

The reaction of iPP with MAH was successfully performed as follows: a four-neck round-bottom glass flask fitted with a dripping funnel, a magnetic stirrer, and a thermometer, MAH (3.00 g, 30 mmol), PP (9.00 g), and dried *O*-xylene as a surface activating agent (80 mL) were mixed in the reaction flask to provide specimens of different graft levels for thermal analysis. The speed of agitation was approximately 90 rpm. In order to form the polypropylene particles, and swell, the temperature was kept at 80 $^oC$ for 90 minutes. Then, (0.4 gr of benzoyl peroxide (B.P.O) dissolved in 9 gr of xylene) was added into the content flask and refluxed under an argon atmosphere for 30 minutes. The reaction was kept at 100 $^oC$ for 3 hours. After the time of reaction was terminated, the obtained (PP-g-MAH) was washed with warm water until pH became 7. Finally, the graft copolymer with acetone was washed and dried at 60–70 $^oC$ for about 25 hours in a vacuum oven. The iPP-g-MAH (2 %) was synthesized with 10 g of MAH [33].

*Synthesis of PP $^-$OH*

A facile method for the synthesis of PP-OH is as follows: A 250-mL glass reactor fitted with a dripping funnel, a reflux condenser and a mechanical stirring bar was charged with iPP-g-MAH (3.6 g, 0.09 mmol MAH) and *o*-xylene (40 ml). Next, iPP-g-MAH was dissolved at 120 $^{o}$C for 5 hours under $N_2$ protection. Then, ethanolamine (40 mL, 0.595 mmol) by the dripping funnel was added drop-wise to the reaction mixture and was refluxed at 110 $^{o}$C for about 5 hours while stirring. Plunging of the reaction mixture into 100 mL of acetone completed the reaction. In order to obtain precipitate, the polymer was collected by filtration, washed with acetone several times and dried in a vacuum oven at 90 $^{o}$C for 10 hours to give hydroxylated polypropylene (PP-OH) in the form of a white powder (Scheme 1).

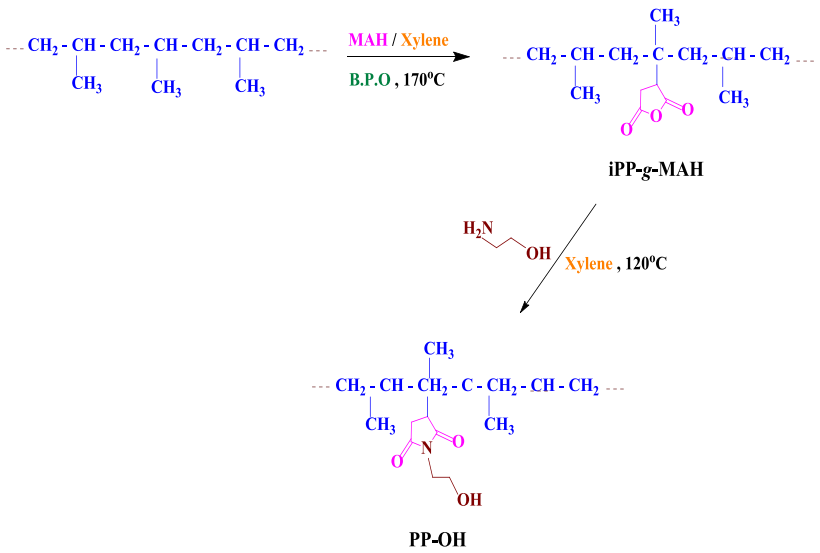


**Scheme 1**. Preparation of maleic anhydride grafted polypropylene (iPP-g-MAH) and hydroxyl group containing PP (PP-OH).

*Synthesis of graft copolymer*

*Preparation of PP-CTA-macro-RAFT agent*

In a 100 mL round-bottom glass flask fitted with a mechanical stirring bar, obtained PP-OH (0.9 g) and xylene (30 ml) were dissolved under flowing nitrogen at 100 $^{o}$C for about 2 hours. After the polymer dissolution, 4-cyano-4-[(phenylcarbothioyl) sulfanyl] pentanoic acid (0.35 gr), DCC (0.03 mL, 0.22 mmol) and DMAP (0.03 mL, 0.02 mmol) were added to the contain flask and the reaction mixture was stirred at 120 $^{o}$C under argon pouring for 5 hours. In order to precipitate, the reaction mixture was plunged into 80 mL of methanol. The resulting precipitates were collected by filtration and dried in a vacuum at 80 $^{o}$C for about 10 hours to obtain 2 gr of 4-cyano-4-[(phenyl carbon thioyl)] solfanyl valeric group containing PP.

*Graft polymerization of styrene onto isotactic polypropylene via RAFT polymerization technique*

To perform this reaction step, 0.2 gr of grafted polypropylene with RAFT agent in 15 mL of xylene was stirred at 60 ° C using a magnetic stirrer under an argon atmosphere. After complete dissolution, 0.01 gr of AIBN imitator and 2 mL of distilled styrene were added into the reaction flask. The polymerization process was performed at 90 °C under argon pouring for 7 hours. After cooling the solution at room temperature, the product obtained was dissolved in xylene and to ice methanol was precipitated and dried in a vacuum oven at 60 °C. The separation of iPP-*g*-PSt from PSt (possibly thermally formed) was performed according to a process introduced by Xie et al [34]. Thus, the raw product was extracted with cyclohexane at 30 °C for several times in order to eliminate PSt. The refined product was dried in a vacuum oven and weighed. The resulting copolymer is a yellow powder (150 mg) (Scheme 2).

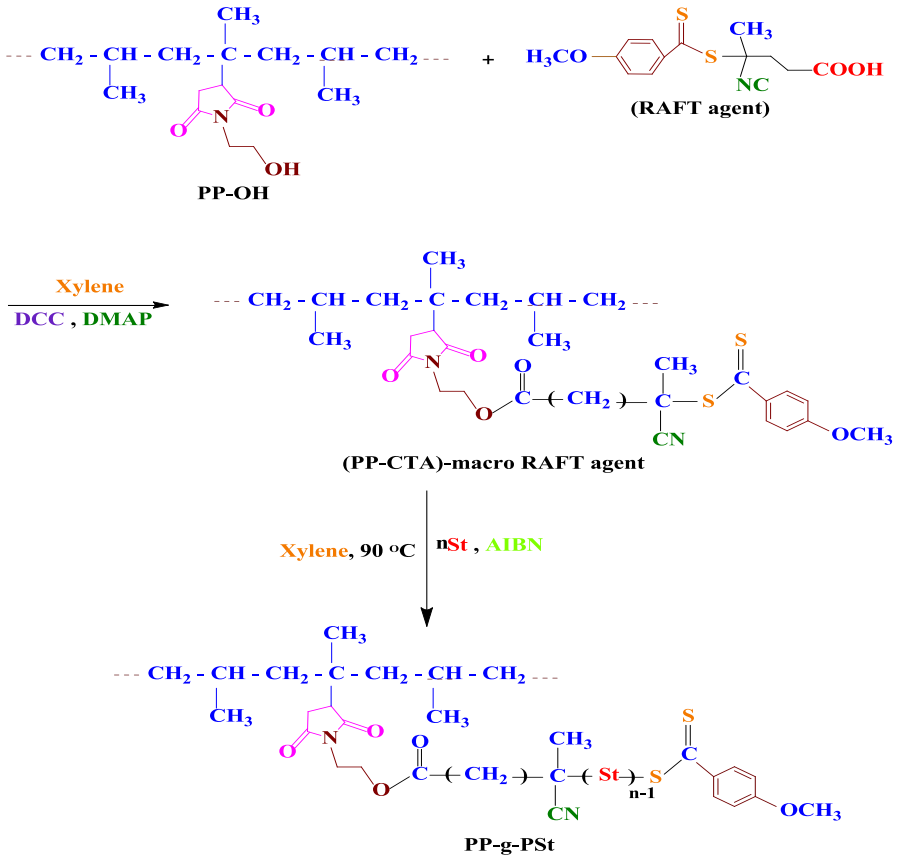


**Scheme 2**. Overall strategy for graft polymerization of styrene onto isotactic polypropylene by RAFT method (b).

*Surface Modification of pristine Montmorillonite*

In order to modify the surface of Montmorillonite, Organophilic montmorillonite (O-MMT) was provided after treatment of hexadecyltrimethyl ammonium chloride salt using an ion-exchange method. For modification, 0.3 gr of clay nanoparticles in 70 mL deionized water were dispersed under ultrasonic waves for 20 minutes. Afterward, the rectifier separately was obtained in deionized water, then the rectifier was added to the mixture by a funnel dropper at a little higher than the CEC (cation exchange capacity) of MMt. After intensely stirring for 10 hours, the resulting suspension was filtered with deionized water several times. Finally, the obtained product was dried at 60° C for about 45 hours, when it was grounded into a powder.

*Preparation of the PP-g-PSt/O-MMT nanocomposite through solution intercalation method*

In this investigation, 0.012 gr of the modified nanoparticles (3 wt %) was dispersed in 50 ml of xylene ultrasonic waves with 80% intensity for 20 minutes. The reaction mixture inside a two-necked flask was equipped with a dripping funnel, a reflux condenser and a magnetic stirrer. It was poured and stirred with a magnetic stirrer for 20-40 minutes in order to be completely homogeneous. Simultaneously, with the gradual temperature increase to 60 °C, 0.5 gr of the synthesized copolymer [iPP-graft-MAH-graft-PSt] dissolved in 50 mL of dry xylene was added drop-wise to the reaction mixture by dripping funnel for about 6 hours. The mixture was refluxed at 80 °C for 20 hours. Finally, the resulting polymer mixture was precipitated in cold methanol and the resulting white precipitates were filtered and dried at room temperature (Scheme 3).

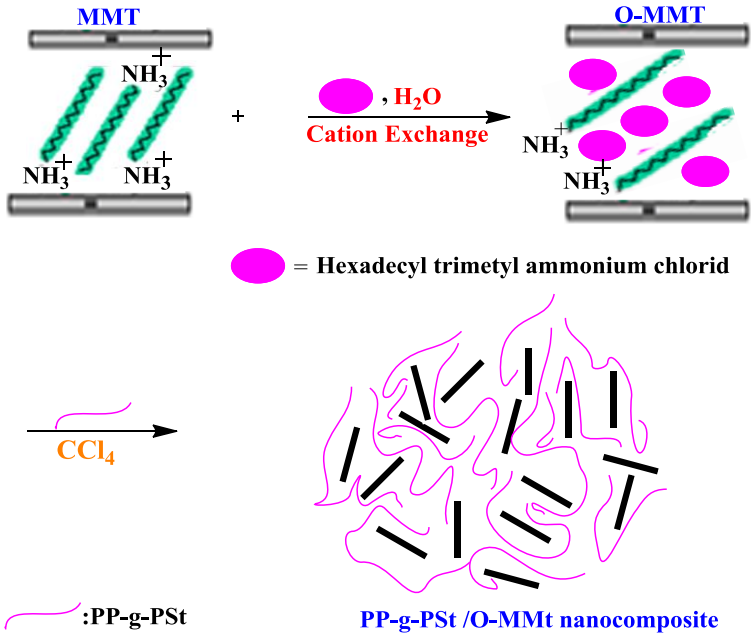


**Scheme 3**. The surface modification of montmorillonite (a) and preparation of PP-*g*-PSt/MMT nanocomposite through solution polymerization (b).

## Result and discussion

*FT-IR (Fourier transform infrared) study*

The RAFT polymerization was activated with radicals which were created from a conventional initiator and progressed by means of living growth produced by the trithiocarbonate RAFT agent or initial dithioester. The preparation of RAFT agent was studied using $^{1}H$ NMR and FTIR spectroscopies. The FT-IR spectrum of bis (4- methoxy diphenyl) dithio peroxy anhydride and 4-cyano-4-[(phenylcarbothioyl) sulfanyl] pentanoic acid appears in Figure 1.

FTIR spectra of bis (4- methoxy diphenyl) dithioperoxy anhydride (Figure 1a) exhibits the absorption peak at 560 $cm^{-1}$ attributable to S-S bending vibration and at 658 $cm^{-1}$ area related to C-S stretching vibration. Also, the absorption peak at 1245 $cm^{-1}$ belonged to the stretch vibration of C-O and 1440 $cm^{-1}$ and 1594 $cm^{-1}$ areas attributable to the stretch vibration of aromatic C=C bond. In FTIR spectrum of 4-cyano-4- [(phenyl carbon thioyl) solfanyl pentatonic acid (Figure 1b), if the favorable compound is synthesized accurately, the vibrations of the C-N, C=O and OH bending of carboxylic acid groups should appear in the spectrum.

By comparison between Figures 1 (a) and (b), it can be seen which three additional absorption peaks become visible at 1762 $cm^{-1}$ to 3200 $cm^{-1}$, which are related to C=O, C-N and OH groups, respectively. There is a small peak at 2320 $cm^{-1}$ which corresponds to the stretch vibration of C-N group. Furthermore, the wide peak of stretching vibration of acidic OH, is observed at 2600 $cm^{-1}$ to $^{3200}$ $cm^{-1}$ which overlapped with stretching absorption of CH at 2996 $cm^{-1}$. The stretch vibration of C=O is observed at 1765 $cm^{-1}$, Also broad peaks at 1440 $cm^{-1}$ and 1595 $cm^{-1}$ are attributed to the stretch vibration of aromatic C=C bond in RAFT regent.

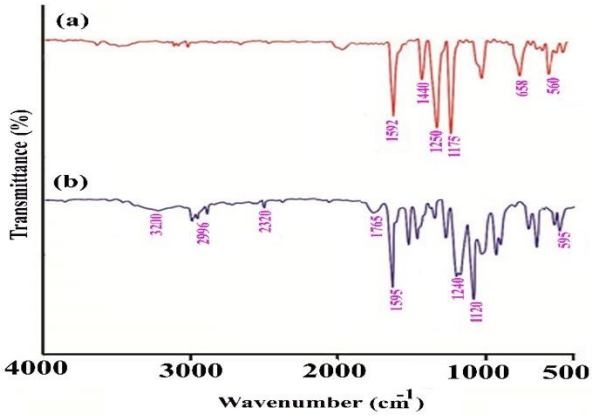


**Figure 1.** The FTIR spectra of bis (4-methoxy diphenyl) dithioperoxy anhydride (a), and 4-cyano-4-[(phenylcarbothioyl) sulfanyl] pentanoic acid (b).

The FT-IR spectrum of iPP (a), iPP-*g*-MAH (b) and PP - OH (c) are shown in Figure 2. The spectrum of iPP-*g*-MAH (b), revealed an intense absorption band at 1735 $cm^{-1}$ that was attributed to the presence of the carboxylic groups. On the other hand, the FT-IR spectrum of iPP (a) indicated that in the range of 1800 $cm^{-1}$ to 2500 $cm^{-1}$ there is no sign of the presence of each peak. This result visibly displayed that in the swell grafting process, the maleic anhydride monomers onto the polypropylene chains were successfully grafted. As shown in Figure 2c, after reaction between iPP and MAH with ethanolamine, the absorption peaks for C=O observed at 1700 $cm^{-1}$ to 1780 $cm^{-1}$ and stretch vibration of OH (hydroxyl) appeared at 3455 $cm^{-1}$. These absorption peaks can be related to a succinimide group, indicating that in comparison with hydroxyl and amino group of ethanolamine, SA group dominantly reacted with the amino group of ethanolamine.

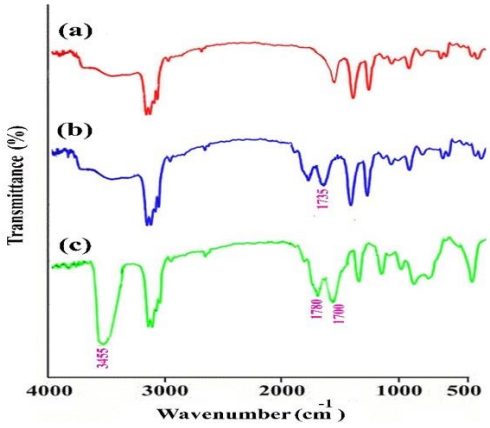


**Figure 2.** The FTIR spectra of pure iPP (a), iPP-g-MAH (b) and iPP-OH (c).

Figure 3 illustrates the FTIR spectra of PP-g-CTA (a) and PP-g-PSt (b). According to Figure 3a, the stretch vibration of C-N which is a small peak, was observed at 2504 cm-1 area. The stretch vibration of C = O is observed at 1725 cm-1. The stretch vibrations of C-S, C = S and C-O also can be seen at 530 cm-1, 1095 cm-1 and 1305 cm-1, respectively. The stretch vibration of aromatic ring is seen at 1595 cm-1. Whereas, the stretch vibrations of S-S bond were seen at 596 cm-1. In Figure 3b, the stretching vibration of C = O in addition to the succinimide group appeared at 1745 cm-1. Furthermore, -CH stretch vibration of aromatic ring was discovered at 3000 cm-1 to 3020 cm-1 and the stretch vibration of methylene was observed around 1496 cm-1. Also, the grafted specimen (Figure 3b) indicated a new band at 696 cm-1 which is related to polymerization of poly (styrene).

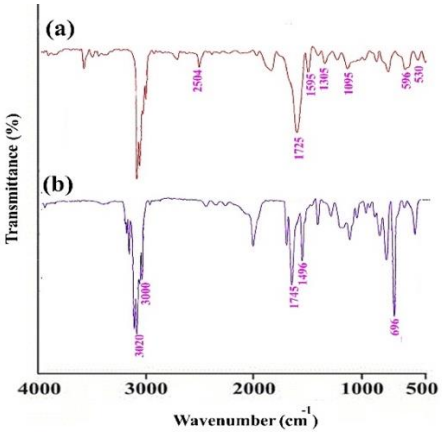


**Figure 3.** The FTIR spectra of iPP- *g*- CTA (a) and PP-*g*-PSt (b).

*$^{1}$H NMR (proton nuclear magnetic resonance) study*

Nuclear magnetic resonance is one of the best spectroscopy methods for identifying organic compounds and investigating of thermal degradation. Many nuclei can be examined by this method, yet carbon and hydrogen are commonly used. The $^{1}$H NMR spectrum of PP-OH, bis (4-methoxy diphenyl) dithioperoxy anhydride and 4-cyano-4- [(phenyl carbon thioyl) sulfanyl pentatonic acid which were carried out in $CDCl_3$ are shown in Figure 4.

According to the $^{1}$H NMR spectrum of PP-OH, two types of aliphatic protons (-N–$CH_2$–$CH_2$–OH) are associated with signals of δ 3.61 and δ 3.64 ppm. The signals of SA ring seen in partly shifted to the higher magnetic field (δ 2.5–3.06 ppm) which indicates that the SA group through the reaction with ethanolamine was conversed to the succinimide group. The relative severities of the signals at 3.64, 3.61, and 2.5–3.06 ppm being virtually evaluated to be 2, 2, and 3 respectively, displaying the presence of the N-(2- hydroxyethyl) succinimide group.

On the other hand, in $^{1}$H NMR spectrum of bis (4-methoxy diphenyl) dithioperoxy anhydride, the peaks are seen at ~7–8 ppm related to the aromatic hydrogens, and the absorption band observed at ~1.8 ppm is owned to remnant water in the obtained product. Accordingly, in 4-cyano-4-[(phenylcarbothioyl) sulfanyl] pentanoic acid, the chemical shifts are seen at 7–8 ppm which is related to the aromatic hydrogens on the benzene ring. The resonance at about 1.0-2.2 and 4.0 ppm are attributed to the aliphatic protons of the sample. Accordingly, the produced spectrum matches the reference spectrum can be seen some impurities (Figure 4).

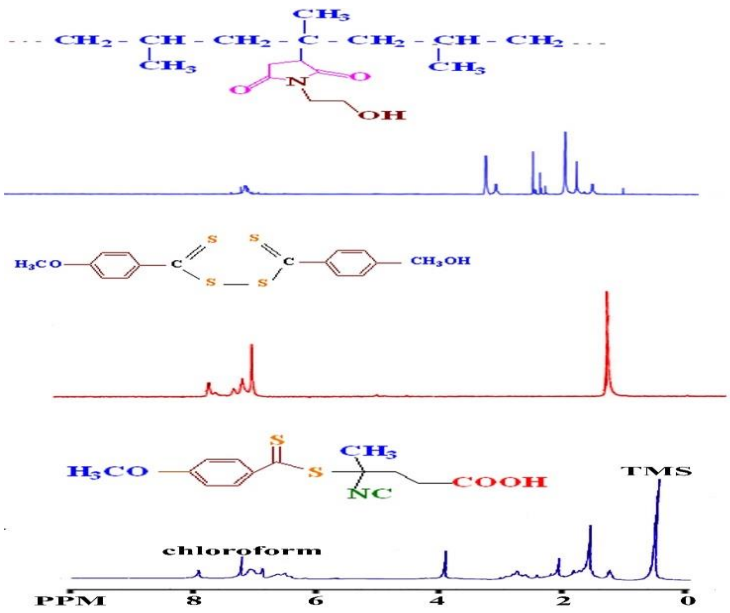


**Figure 4**. The $^{1}$H NMR spectra of iPP-OH, 4-cyano-4-[(phenylcarbothioyl) sulfanyl] pentanoic acid and bis (4-methoxy diphenyl) dithioperoxy anhydride recorded in solvent $CHCl_3$.

*Thermal property study*

*TGA study*

The thermal degradation of the synthesized specimens was investigated by TGA (thermogravimetric analysis) that was created during the period of heating under nitrogen flowing for iPP, iPP-g-MAH, PP-*g*-PSt and PP-*g*-PSt/ MMT nanocomposites (3 wt %) are shown in Figures 5 and 6. Generally, there appear two stages of weight loss, which start at 100°C and end at 600°C, which may be attributed to the degradation of intercalating agent chased by the structural decomposition of the polymers. As seen in Figure 5, there are two mass-loss processes before at 600 $^{o}$C. The first mass-loss process is observed at 210-220 $^{o}$C and the second mass-loss in temperature at 400 $^{o}$C which is related to the thermal degradation of polymer. As can be seen, after the grafting copolymerization reactions, there were no considerable changes in thermal stability.

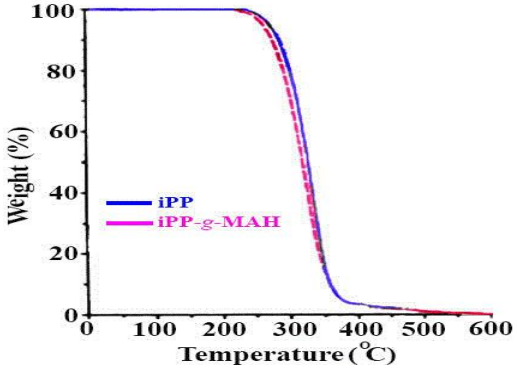

**Figure 5.** TGA trace of pure iPP and iPP-g-MAH.

On the other hand, The TGA curves of PP-*g*-PSt and PP-*g*-PSt/ MMT nanocomposites (3 wt %: The weight of clay in the nanocomposite is 3%) are shown in Figure 6. The main thermal decomposition with weight loss of 86 wt. %, resulted from the degradation of the polymer chains. In Figure 6, the specimens displayed a beginning temperature of decomposition at about 310 – 350 $^{o}$C and was decomposed at above 450$^{o}$C. When the clay was homogenously dispersed onto PP-*g*-PSt, it showed one obvious degradation stages. The degradation stage for PP-*g*-PSt occurred at 350 $^{o}$C which was attributed to the degradation of PP. The distribution of clay into the pristine copolymer mixed both degradation peaks into a sharp peak at 450 $^{o}$C. Furthermore, when the grafted copolymer was present, the sharp degradation peak shifted to a higher temperature (450 $^{o}$C). This is due to the additional intense interactions between clay and grafted copolymer rather higher than PP.

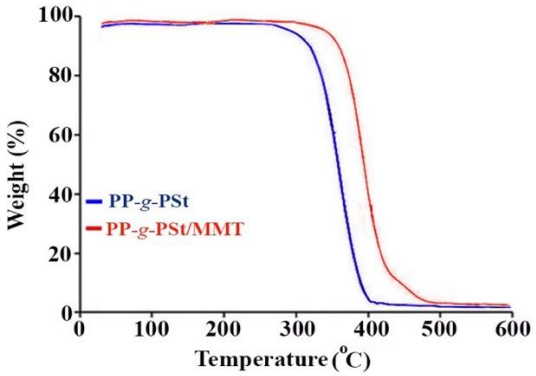


**Figure 6**. TGA results of PP-*g*-PSt and PP-*g*-PSt/ O-MMT nanocomposites.

*DSC study*

DSC was employed to define transition temperatures consisting of decomposition, glass transitions and melting cross-linking reactions. However, it evaluated just the entire heat process indicating the totality of thermal transitions in the specimen. The thermal behavior of iPP, iPP-*g*-MAH and PP-*g*-PSt, PP-*g*-PSt/MMT nanocomposite were also studied using DSC as shown in Figure 7. Accordingly, the melting temperature (*Tm*) of iPP (161 $^{o}$C) was partly higher than those of iPP-g-MAH (160 $^{o}$C) and AH (heat of fusion) (107 J/g). The results indicated that the extent of (AH) decreased with an increase in grafting. It was possibly because of the grafted branches, which disordered the order of the chain structures in iPP and increased

the spacing between the chains; as a result, the percent crystallization, and moreover (AH), reduced [35].

For the DSC trace of PP-g-PSt hybrids, the thermogram of each specimen was collected in the second heating continuity at 10 $^{o}$C min$^{-1}$ in order to remove the thermal history. In all materials, it was obvious that the peak *Tm* at around 160 $^{o}$C displayed the PP segments in the backbone and with increasing styrene value of the hybrid. The heat of fusion (AH) progressively decreased.

Despite the increasing value of the styrene, the relative crystallinities of the PP phase in the hybrids are almost fixed. In the produced PP-*g*-PSt, two T*g* at 30 $^{o}$C and 150 $^{o}$C were seen. This value displays the presence of microphase separation in this graft copolymer. This has been an expected result because it is obvious that polystyrene is immiscible with polypropylene [35]. In the DSC trace of PP-*g*-PSt/MMT nanocomposites, the value of the *Tg* (glass transition temperature) is 90 $^{o}$C, which is partly higher than that of neat iPP. The DSC curve of PP-g-PSt/MMT nanocomposite indicates that the decomposition of the nanocomposite obtains in two stages: the first stage assigned to the decomposition of the PP chain (120-155 $^{o}$C), and the second stage is attributable to PSt chain scission (200-340 $^{o}$C). Empirically, this is attributed to the restriction of the polymer chains adjoining to the clay layers, which is a barrier for segmental movement of the polymer chains. Since O-MMT layers are distributed in the polymer matrix on a nanoscale, intense interfacial forces which are formed between the polymer chains and the silicate layers, may restrict the motion of chain segments, that leading to the temperature decomposition and enhancement in *Tg*. Assuming an inorganic material, the extraordinary thermal particularity of MMT can be quietly indicated; this led to progress in the heat persistence of the nanocomposite, which is clear with an increase of O-MMT.

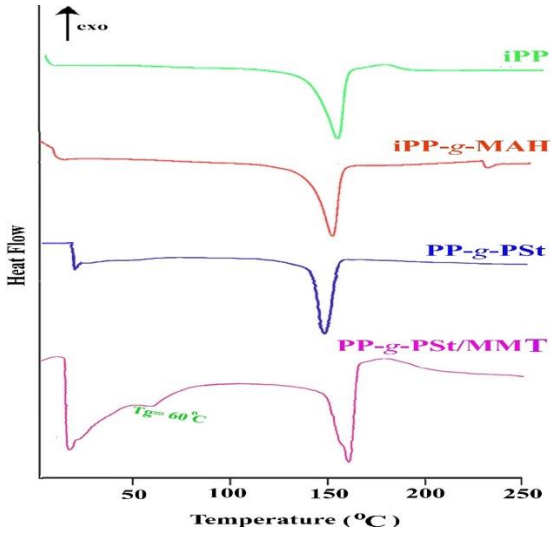

**Figure 7.** DSC trace of pure iPP and iPP-*g*-MAH and PP-*g*-PSt and PP-*g*-PSt/ O-MMT nanocomposite.

*Morphology Study*

Obviously, scanning electron microscopy (SEM) was utilized for the investigation of microstructure and distribution of nanofiller within the polymer matrix. The conversions of stage morphology of the fractured cross portion of the synthesized PP-g-PSt/O-MMT nanocomposite are shown in Figure 8. This Figure exhibited the fracture and folded morphology of the PP-g-PSt/ clay nanocomposite. These images also have proved the fragmented structure of synthesized nanocomposite. From the Figure 8, we can conclude that with the increase of nano-clay, the cohesion between the two components developed to make a homogeneous morphology. Thus, the developed homogeneity morphology increases the tensile and flexuous particularities. Also, after grafting PSt onto PP backbone the surfaces of the sample (PP-g-PSt) demonstrated relatively rough with some bulge, owing to grafting processes.

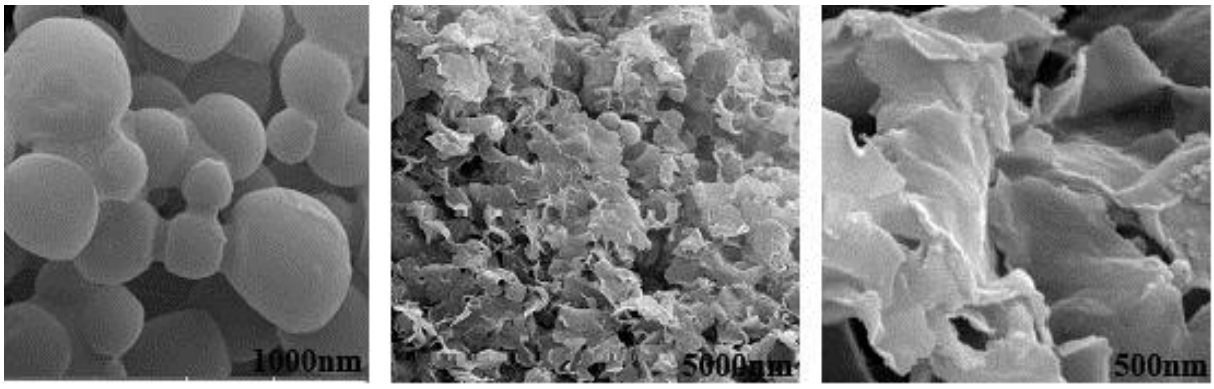


**Figure 8.** The SEM image of PP-*g*-PSt/ MMT nanocomposite.

## Conclusion

A well-defined, PP-*g*-PSt/MMT nanocomposite was synthesized using a versatile method via the RAFT method. The preparation of PP-*g*-PSt graft copolymer using FTIR and $^{1}$H NMR analysis, was successfully demonstrated. The SEM images indicated that the growth of PSt onto iPP resulted in folded and wrinkled morphologies since the grafting occurs chiefly at the surface of polymer. As a result, SEM images proved the dispersion of polymers on nanoparticle surfaces. The successful synthesis of the above-mentioned materials was demonstrated using TGA and DSC analysis. TGA results displayed a bigger increase in thermal particularity of

resultant composite than those of neat copolymer. DSC results disclosed the increase in *Tg* of resultant composite compared to pristine copolymer. In conclusion, we imagine that the synthesized PP-*g*-PSt/O-MMT nanocomposite may be realized applications as membrane materials, fortifying agents in polymer composite materials, packaging materials, etc.

**References**

[1] N.F. Himma, S. Anisah, N. Prasetya, I. G. Wenten, *J. Polym. Eng*., 36, 0112 (2015).

[2] D. Li, Y. Shi, L. Yang, L. Xiao, D. K. Kehoe, Y. K. Gun'ko, J. J. Boland, J. J. Wang, *Nature Food*, 1, 746 (2020).

[3] W. Hufenbach, R. B€ohm, M. Thieme, A. Winkler, E. M€ader, J. Rausch, M. Schade, *Mater. Des*, 32, 1468 (2011).

[4] H. G. Ock, D. H. Kim, K. H.Ahn, S.J. Lee, J. M. Maia, *Eur. Polym. J*., 76, 216 (2016).

[5] S.Wang, L.Wang, B.Wang, H. Su, W. Fan, X. Jinga, *Polymer*, 233, 124214 (2021).

[6] Y. Wang, K. Gu, A. Soman, T.Gu, R. A. Register, Y.L. Loo, R. D. Priestley, *Macromolecules*., 53, 5740 (2020).

[7] H. Mardani, H. R. Mamaqani, K. Khezri, M. S. Kalajahi, *Applied Physics A*., 126, 251(2020).

[8] Y. Wadaa, T. Kobayashi, H. Yamasaki, T. Sakata, N. Hasegawa, H. Mori, Y. Tsukahara, *Polymer*, 48, 1441 (2007).

[9] E. V. Kolyakina, A. B. Alyeva, E. V. Sazonova, E. A. Zakharychev, D. F. Grishin, *Polym. Sci B*., 62, 328 (2020).

[10] N. Naga, M. Sato, K. Mori, H. Nageh, T. Nakano, *Polymers*, 12, 2047 (2020).

[11] X. Wang, L. Chen, L. Wang, Q. Fan, D. Pan, J. Li, F. Chi, Y. Xie, S. Yu, C. Xiao, F. Luo, J. Wang, X. Wang, C. Chen, W. Wu, W. Shi, S. Wang , X. Wang, *Sci. China. Chem*., 62, 933 (2019).

[12] N. Corrigan, K. Jung, G. Moad, C. J. Hawker, K. Matyjaszewski, C. Boyer, *Prog. Polym. Sci.*, 111,101311 (2020).

[13] P. R. Rodrigues, S. A. Gonçalves, R. P.Vieira, *Eur. Polym. J*., 147,110303 (2021).

[14] R. Zeng, Y. Chen, L. Zhanga, J. Tan, *Polym. Chem*., 11, 4591 (2020).

[15] L. Mrah, R. Meghabar, *N Appl. Sci*., 2, 659 (2020).

[16] T.F.Menéndez, D.G.López, A.Argüelles, A. Fernández, J.Viña, *Polym. Test*., 90, 106729 (2020).

[17] M. A. Aldosari, K.B.B. Alsaud, A. Othman, M. A. Hindawi, N. H. Faisal, R. Ahmed, F. M. Michael, M. R. Krishnan, E. Asharaeh, *Polymers*., 12, 1155 (2020).

[18] H. Zhang, *Eur Polym J*. 49, 579 (2013).

[19] M. Jaymand, M. Hatamzadeh, Y. Omidi, *Prog. Polym. Sci*., 47, 26 (2015).

[20] A.A. Entezami, M. Abbasian, *Iran. Polym. J*., 15, 583 (2006).

[21] M. Abbasian, M. Seyyedi, M. Jaymand, *Polym. Bull*., 77, 1107 (2020).

[22] B. Massoumi, M. Abbasian, R. Mohammad-Rezaei, A. Farnudiyan-Habibi, M. Jaymand, *Polym. Adv. Technol*., 30, 1484 (2019).

[23] R. Mohammad-Rezaei, B. Massoumi, M. Abbasian, M. Eskandani, M. Jaymand, *J. Mater. Sci: Mater Electron*, 30, 2821 (2019).

[24] M. Abbasian, L. Razavi, M. Jaymand, S. Ghasemi Karaj-Abad, *Scientia*, *Iranica*, 26, 1447 (2019).

[25] M. Abbasian, M. Judi, F. Mahmoodzadeh, M. Jaymand, *Polym. Adv. Technol*., 29, 3097 (2018).

[26] R. Mohammad-Rezaei, B. Massoumi, M. Abbasian, M. Eskandani, M. Jaymand, *J. Mater. Sci*., 30, 2821 (2019).

[27] S. Ghasemi Karaj-Abad, M. Abbasian, M. Jaymand, *Carbohydr. Polym*, 152, 297 (2016).

[28] M. Barsbay, O.Güven, *Rad.Phys.Chem*, 169, 107816 (2020).

[29] G. Moad, Aust. *J. Chem*., 59, 661 (2006).

[30] D. HyoungKim, H.SungKim, Compos. Sci, Tech., 101, 110 (204).

[31] M. Abbasian, F. Mahmoud Zade, *J. Elastom. Plast*, 49,173 (2017).

[32] Le, T., et al., "editors. PCT Int. Appl. WO 9801478 A1 980115" *Chem. Abstr.*, (1998).

[33] T. KO, P. Ning, *Polym. Eng. Sci*., 40, 1589 (2000).

[34] H.Q. Xie, Z.S. Liu, J.S. Guo, *Polymer*, 35, 4914 (1998).

[35] Q. Xiea, N, Liua, D. Lin, R. Qua, Qi. Zhou, F.Gea, *Env Pollu*., 263,114102 (2020).

[36] L. Zhang, G. Fan, C. Guo, J. Dong, Y. Hu, M. Huang, *Eur. Polym. J*., 42, 1043 (2006).